Implementation and mechanical characterization of 2nm thin diamond like carbon suspended membranes

Anne Ghis, Nawres Sridi, Marc Delaunay, Jean Christophe Gabriel

Implementation and mechanical characterization of 2 nm thin diamond like carbon suspended membranes

Anne Ghis [a,*], Nawres Sridi [a], Marc Delaunay [b], Jean-Christophe P. Gabriel [b]

[a] Univ. Grenoble Alpes, F-38000 Grenoble France CEA, LETI, MINATEC Campus, F-38054 Grenoble, France
[b] Univ. Grenoble Alpes, F-38000 Grenoble France CEA INAC-SP2M, F-38054 Grenoble, France

ARTICLE INFO

ABSTRACT

Ultrathin diamond like carbon (DLC) layers with thickness down to 2 nm have been integrated into suspended membranes enabling their mechanical properties to be characterized.

The goal of this study is the integration of a membrane with micrometric suspended area into operational MEMS. The early structure for feasibility study of a device is made of a membrane suspended above a micrometer sized cavity. Deflection is electrostatically induced by applying an electric potential between the membrane and the floor of the cavity. The thickness of the membrane determines at first order the amplitude of the deflection. Experimental measurements are presented and results obtained discussed. The experimental bending rigidity value is extracted and is shown to be a key parameter for modeling membrane's behavior in any other mechanical embodiment.

DLC is identified as a suitable material for free standing over a micrometer large area, even when only a few nanometers thick, and a promising candidate for MEMS integration.

© 2015 Elsevier B.V. All rights reserved.

1. Introduction and objectives

Micromachined ultrasonic transducers (MUT) are suitable sensors for acoustic probing in non-solid media [1,2]. Their spatial resolution currently addresses several tens of micrometers. In order to further improve it the transducer active area must be downsized down to the micrometer range. To reach this goal various challenges must be addressed regarding various aspects such as materials used, their technological processing, readout electronics, and acoustic phenomena. This paper reports results of our investigations into the suitability of nanometer thick diamond like carbon (DLC) free standing layers in regard to those challenges.

Diamond like carbon has drawn attention in the past for its wear and electrochemical properties [3,4]. For MEMS applications, DLC has been mainly identified as a good candidate for coating layers [5] due to its low roughness that reduces friction between mobile parts. Furthermore, the Young's modulus of some carbon materials has been reported to range from a few tens of MPa to more than 1 TPa, depending on thickness and atom arrangement [6–8]. This triggered our interest in carbon materials, beyond graphene and its sp2 carbon hybridization, and hence into DLC as a core material for MEMS and not just for simple coatings [9].

Mechanical properties of ultrathin DLC have been studied by Suk [10]. The DLC film was deposited onto a TEM grid and an AFM was used to apply a stress and measure the resulting deflection [11]. The Young's modulus was discussed with regard to the initial stress that the deposition process could have set on the membrane.

The present study is a device-oriented approach that considers the feasibility and advantages of using freestanding nanometer thick DLC as a vibrating membrane in acoustic MEMS. Skipping over the intrinsic structure and properties of the material, we focus on the final membrane properties, as results from the whole integration process, after implementation into an operational device.

Preliminary results of the integration of a freestanding nanometer thin DLC layer as the mobile part of a MEMS device are presented, together with the determination of the actual membrane properties allowing the design of MEMS with reliable features.

2. Membranes for MEMS at the micron scale

Micromachined ultrasonic transducers (MUT) basically consist in a flexible membrane suspended above a cavity. It may either generate pressure variations if actuated, or be deflected by incident pressure. In the case of capacitive MUT, the membrane and the floor of the cavity are designed to act as the two plates of an electrical capacitor. When operated as a pressure generator, an applied bias voltage induces the membrane deflection. When operated as a sensor, a variation in

---

incident pressure induces a change in the capacitance value. The amplitude of the membrane deflection determines the dynamic range and the sensibility of the transducer.

The thickness of the suspended membrane is a key parameter in the determination of the membrane deflection. When the suspended length is in the micrometer range, a thickness limited to a few nanometers is needed in order to obtain signals with detectable amplitude.

This specifies the requirement for flexible and self-standing material, even in nanometer thicknesses, and also with sufficient electrical conductivity for acting as a capacitor plate.

Here, it should be noted that the Young's modulus is a bulk material property that is typically used to model and design mechanical devices. It therefore cannot be used in the case of a few atom thick membranes. Indeed, they do not behave as bulk since, at this nanoscale, surface effects might dominate together with alterations due to synthesis and integration processes. Furthermore, modeling calculation's results are highly dependent on the true thickness of the layer as well as of the built-in stress that are usually not known with the required accuracy. Hence, such modeling may be damaged by these uncertainties, which renders devices' design hazardous.

In this study we consider that the key parameter for modeling such devices is the bending rigidity D. The classical formulation of D, when there is no built-in stress in the considered layer, is given in Eq. (1):

$$D = \frac{E \cdot e^3}{12 \cdot (1-\nu^2)} \tag{1}$$

where e is the layer's thickness, E is the bulk material Young's modulus, and ν is the Poisson's coefficient. Since (i) bending rigidity is representative of the membrane's behavior whatever the geometrical embodiment and that (ii) it can experimentally be obtained by AFM measurements of the spring constant on an early membrane realization, bending rigidity is the parameter that allows for modeling devices with true membrane description, and thus more accurately than by downsizing from bulk material's properties.

The present work describes the determination of the bending rigidity of 2 nm thin DLC self-standing membranes, as well as of DLC/metal hybrid membranes.

3. Test device realization

DLC is obtained by Electron Cyclotron Resonance (ECR) [12,13]. ECR sputtering plasma sources enable the production of thin films of diamond like carbon (DLC) on a substrate [14]. In our case, the DLC deposition process is carried out using a 20 cm^2 graphite target biased at a 400 V dc negative voltage in a low pressure Krypton plasma (5.10^{-4} mbar) assisted by 2.45 GHz microwaves. XPS analyses showed a rate of 25% of sp^3 bonds in the resulting thin films.

The growth rate is 20 nm in 60 min. Because of the difficulty to accurately measure ultra-thin layers' thicknesses, we first approximate that
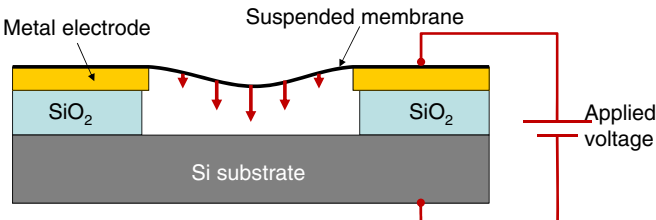

Fig. 2. SEM picture of a 10 nm thick DLC membrane after report, suspended above a 1.4 μm large, 300 nm deep trench. The DLC layer appears tight. The surface texture that can be observed for the DLC is the conformal image of the sacrificial layer's surface on which it was first grown.

the carbon deposition's thickness is proportional to the duration of the plasma lightening.

The test device consists in a doped silicon substrate covered with 200 nm of thermal silicon dioxide and covered with a 100 nm thick CrAu layer deposited on top. SiO$_2$ and CrAu layers are then patterned in order to provide a set of 300 nm deep trenches. Several trench widths ranging from 1 μm to 2 μm are available on the test devices (Fig. 1).

The DLC layer is deposited by a stamping approach: for this a secondary substrate is used that is first coated with a sacrificial layer onto which DLC is grown. Then this secondary substrate is stamped onto the test device and the sacrificial layer removed. The DLC layer is therefore fully reported onto the test device. This approached enables the making of self-standing membranes above the trenches (Fig. 2).

DLC layers being insulators, in order to electrically actuate the membranes a nickel ECR deposition has also been deposited on top of it in order to produce a hybrid Ni/DLC bilayer. In this case, after its reporting onto the test device, the nickel coat is therefore facing the floor of the trench. Two nickel thicknesses have been used, with average values, estimated from the plasma duration, of 2 nm and 4 nm. A more precise measure of their thicknesses could not be achieved as the topology of the underlying sacrificial layer hindered its measurement by AFM. We therefore cannot exclude a possible inhomogeneity of nickel layers' thicknesses at the nanometer scale.

Fig. 1. Schematic cross-section of the test device, equipped with a membrane. A stack of SiO$_2$ (200 nm) and CrAu (100 nm) layers is deposited onto a highly doped Si++ substrate, and then patterned to delimit wedges and trench. Trench widths range between 1 μm and 2 μm. Red arrows represent the electrostatic pressure when a DC voltage is applied between the membrane and the conducting doped silicon floor of the trench.
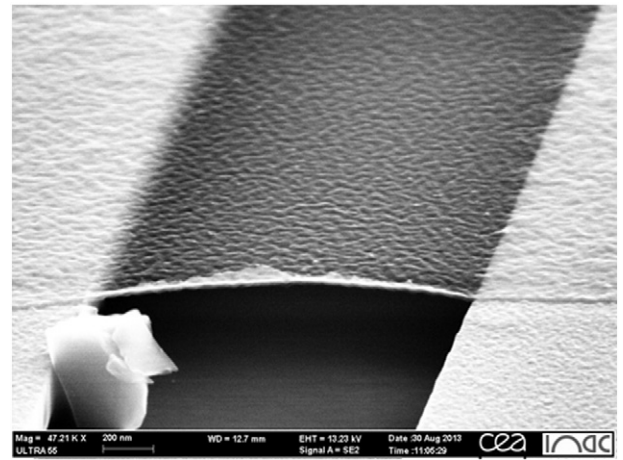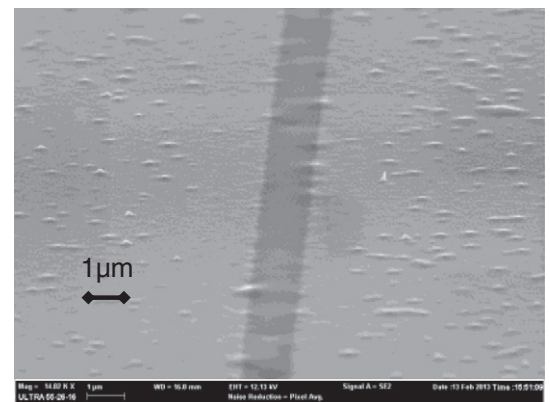

Fig. 3. SEM picture of a 1.2 μm large trench after the report of a Ni/DLC membrane (2 nm Ni + 2 nm DLC). The small bumps are caused by underlying residues. The membrane is partially transparent to the electrons, an indication of its small thickness and suspended nature.
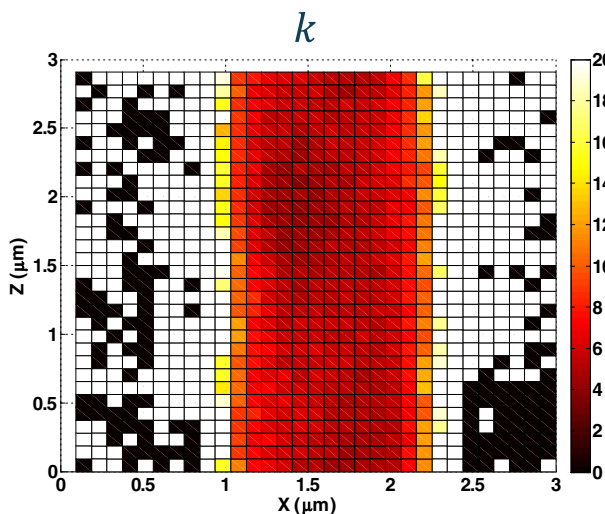
Fig. 4. Spring constant map $k_m(i, j)$ of a membrane suspended above a 1.2 μm large trench. Using an AFM in force mode a 3 μm × 3 μm zone has been probed resulting in a 32 × 32 points matrix of the spring constant values $k_r(i, j)$. The spring constant of the membrane itself $k_m(i, j)$ has been extracted from the rough measurement $k_r(i, j)$ using the relation $k_m(i, j) = \frac{k_c \cdot k_r(i,j)}{k_c - k_r(i,j)}$, where k_c is the spring constant of the AFM cantilever. For the points (i,j) where the membrane is not suspended, the measured spring constant $k_r(i, j)$ is equal to the cantilever spring constant. In this case, the calculation of $k_m(i, j)$ results in a division by 0, the corresponding points thus appear as black ($-\infty$) or white ($+\infty$) on the map.

Following this process, membranes of DLC with 10 nm, 5 nm, and 2 nm thicknesses, and membranes of bilayers 2 nm DLC/4 nm nickel have been realized (Fig. 3).

At this time, the membrane's stress is highly dependent on the report method. We assume the stress to be uniform over the whole area covered by the membrane, which usually encompasses several trenches. In the following, we measure the characteristics of each of the membranes, without making assumptions about compressive or tensile stress in the layer.

4. Membrane actual mechanical parameter determination

For each of the tested devices, local spring constants have been measured on sets of 32 × 32 points using an AFM in force mode, to map a square zone of 3 μm × 3 μm including both wedges of the trench. After correction of the values from the contribution of the AFM cantilever, the local spring constants of the membrane are obtained; an example of the resulting map is shown Fig. 4.

The spring constant at the center of the membrane k_{m0} is the average value of the 32 values of the spring constants $k_m(i_0,j)$ taken at the points situated in the middle of the trench. The standard deviation of the $k_m(i_0,j)$ values is given in Table 1.

From these values, we calculate the spring constant at the center of each of the tested membranes.

The relationship (Eq. (2)) between the spring constant k_{m0} at the center of the membrane suspended between long trench wedges and the corresponding bending rigidities has been established by Sridi et al. [15]. Suspended membranes have been modeled as rectangular, elastic, homogeneous, isotropic, thin plates clamped along their long edges and free along their short edges l.

$$k_{m0} = 137 \frac{D}{l^2} \qquad (2)$$

We then obtained the bending rigidity of the tested membranes. The values, reported in Table 1, range from $3 \cdot 10^{-14}$ N·m to 10^{-13} N·m.

5. Electrostatic deflection

To confirm the relevance and validity of our approach, we compared the results of a calculation performed using the deflection stiffness modulus thus determined, with a direct measure of deflection under equivalent conditions.

We selected a 1.8 μm large trench equipped with a membrane made of a bilayer of nickel (4 nm) and DLC (2 nm). The bending rigidity of this membrane has been determined using the spring constant mapping of a 1.6 μm large trench: $D = 9.9 \cdot 10^{-14}$ N·m (Table 1).

For the experimental determination, the gold wedges of the selected trench and the substrate have been electrically connected by wire bonding, so that a DC voltage can be applied between the membrane and the floor of the trench. The membrane and the AFM probe tip were both connected to the ground.

A first measurement of the profile of the membrane across the trench has been made at 0 V bias voltage between the membrane and the doped silicon floor. A slight depression of 40 nm at the center has been detected. Then, a DC voltage has been applied between the Si++ floor of the trench and the membrane. Profiles of the deflected membrane are measured for 10 V, 20 V, and 30 V of applied voltage (Fig. 5). Differences between the 0 V profile and the biased profiles represent deflections of the membrane across the trench, due to the DC voltage bias (Fig. 6).

Finite element two dimensional modeling has been conducted using a linear elastic material model coupled with an electrostatic one. The experimental bending rigidity $D = 9.9 \cdot 10^{-14}$ N·m and the initial profile are taken into account. A DC voltage is applied between the floor of the 1.8 μm trench and the membrane. At the center of the membrane, the calculated deflection amplitudes are 7 nm for 10 V bias, 15 nm for 20 V bias, and 20 nm for a 30 V bias. The resulting deflection profiles are also plotted in Fig. 6.

The modeled deflection profiles fit the experimental profiles. This confirms bending rigidity value experimentally obtained for this membrane.

Table 1
Experimental spring constants for tested DLC monolayers and Ni/DLC bilayers, and extracted bending rigidity values.

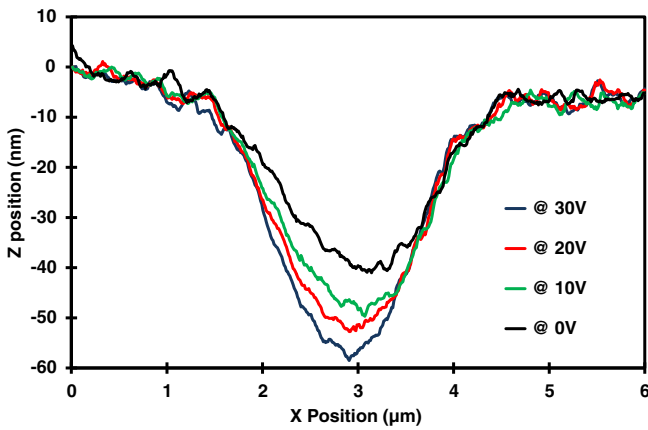| Material	Trench width l (μm)	Spring constant k_{m0} (N/m)	Std. dev σ (k_{m0}) (%)	Bending rigidity D (10^{-14} N·m)
DLC (2 nm)	1.2	3.5	9	3.6
DLC (2 nm)	1.2	3.7	6	3.9
DLC (5 nm)	1.2	3.8	9	4.0
DLC (10 nm)	1.2	7.0	10	7.3
Ni (4 nm) + DLC (2 nm)	1.6	5.3	7	9.9
Ni (2 nm) + DLC (5 nm)	1.4	7.6	10	10.8
Ni (4 nm) + DLC (5 nm)	1.6	5.8	8	10.8

Fig. 5. AFM measurements of a Ni/DLC bilayer (4 nm Ni + 2 nm DLC), suspended above a 1.8 µm large trench. Measurements are taken for different values of the DC potential (0 V, 10 V, 20 V, and 30 V) applied between the membrane and the Si++ floor of the trench. The scan is operated perpendicularly to the trench (X direction), and includes both wedges. It can be noted that the membrane's profile is curved even at 0 V, this initial depression suggests that this membrane is not highly stretched.

6. Results analysis

Bending rigidity values experimentally obtained for the set of implemented membranes of ultrathin DLC and bilayers Ni/DLC membranes, lead us to several considerations.

First, for the DLC monolayers, bending rigidities don't follow the theoretical dependence with the cube of the supposed thickness of the layer. This may be linked to the uncertainty of the actual thickness, as it has been only estimated with regard to the deposition time. It may also be due to predominant surface effects.

The second point to notice is the effective contribution of the nickel coating to the membrane rigidity, although nickel is a priori softer than DLC.

The third point is related to the either compressive or tensile stress of the reported layer. The stress contributes to the bending rigidity value. In this study, although the built-in stress contribution is not assessed, relevant modeling has been carried out.

The values of bending rigidity of the DLC monolayers and of the Ni/DLC bilayers could not be simply calculated from the characteristics of bulk materials, even if the thicknesses had been precisely known.
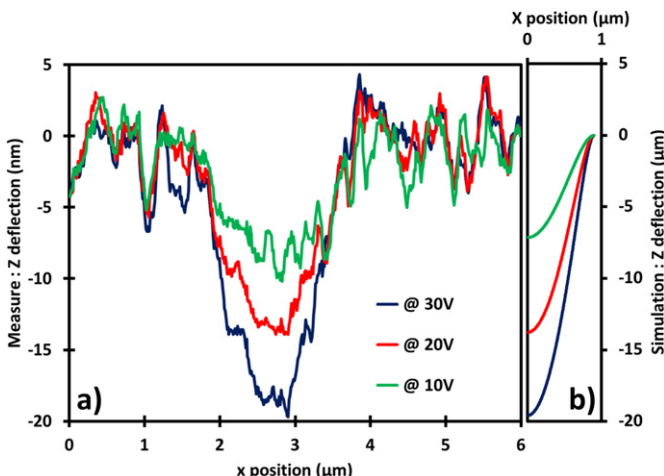
For comparison, let's consider the Young's modulus of 1.1 TPa obtained in the literature [4–6] for a diamond membrane: the value of the bending rigidity of a 6 nm thick membrane, without built-in stress, calculated using Eq. (1) is about $2 \cdot 10^{-14}$ N·m. If this value had been used to model the electrostatically induced deflection of the membrane, the deflection amplitudes would have been overestimated (45 nm for 20 V bias with $D = 2 \cdot 10^{-14}$ N·m).

This remark do not allow for a conclusion related to the Young's modulus of the Ni/DLC composite material, as Young's modulus is a bulk property. The bending rigidity measured after integration of the membrane into a device is influenced by the whole embedding process, namely built-in stress and surface alteration.

The experimental bending rigidities are the specific properties of the membranes as made, and are free from the geometrical configuration. They are key for realistic modeling of the membrane mechanical behavior and allow for MEMS device design with relevant estimation.

7. Conclusion

The DLC we have synthesized using the ECR process and transferred by a stamp method, exhibits original mechanical properties of strength and consistency even in ultra-thin layers. Free standing membranes of a few nanometers thick can be suspended on lengths of several micrometers, and their elasticity permits a significant deformation under the action of applied electrostatic pressure. They can be integrated in microelectronic devices, using conventional techniques, and optionally combined with other materials to produce multilayer having specific properties.

This compliance indicates this material to be compatible with the production of thin membranes for MEMS applications. We described the preliminary mechanical characterization that is needed to extract actual parameters to feed design and modeling.

Prime novelty statement

Prime novelty in the work described in the manuscript "Implementation and mechanical characterization of 2 nm thin diamond like carbon suspended membranes" (Ghis, Sridi, Delaunay, Gabriel) lies in the resolutely pragmatic approach for integrated membrane mechanical characterization.

The bending rigidity values obtained for DLC membranes with nanometric thickness could not have been derived from bulk values.

These values indicate nanometric DLC as a highly relevant material for MEMS applications.

Fig. 6. a) deflection of the Ni/DLC bilayer (4 nm Ni + 2 nm DLC), calculated from measurements presented in figure 5: the 0 V profile has been subtracted from the 10 V, 20 V, and 30 V profiles. b) Deflection calculated by modelling using the bending rigidity experimentally obtained, for applied potential of 10 V, 20 V and 30 V. Only half of the symmetric geometry has been calculated and drawn.

References

[1] A.S. Savoia, G. Caliano, M. Pappalardo, A CMUT probe for medical ultrasonography: from microfabrication to system integration, IEEE Trans. Ultrason. Ferroelectr. Freq. Control 59 (6) (June 2012) 1127–1138. http://dx.doi.org/10.1109/TUFFC.2012.2303.

[2] D. Gross, M. Perroteau, D. Certon, C. Coutier, M. Legros, Fabrication and characterization of wafer-bonded cMUT arrays dedicated to ultrasound-image-guided FUS, Ultrasonics Symposium (IUS), 2014 IEEE International, Sept. 3–6 2014, pp. 181–184. http://dx.doi.org/10.1109/ULTSYM.2014.0046 (vol., no.).

[3] K. Bewilogua, D. Hofmann, History of diamond-like carbon films — from first experiments to worldwide applications, Surf. Coat. Technol. 242 (March 15 2014) 214–225. http://dx.doi.org/10.1016/j.surfcoat.2014.01.031 (ISSN 0257-8972).

[4] Aiping Zeng, V.F. Neto, J.J. Gracio, Qi Hua Fan, Diamond-like carbon (DLC) films as electrochemical electrodes, Diam. Relat. Mater. 43 (March 2014) 12–22 (ISSN 0925-9635).

[5] T.S. Santra, T.K. Bhattacharyya, P. Patel, F.G. Tseng, T.K. Barik, Diamond, diamond-like carbon (DLC) and diamond-like nanocomposite (DLN) thin films for MEMS applications, in: Nazmul Islam (Ed.), Microelectromechanical Systems and Devices, InTech, 2012 http://dx.doi.org/10.5772/29671 (ISBN: 978-953-51-0306-6).

[6] A.C. Ferrari, J. Robertson, Raman spectroscopy of amorphous, nanostructured, diamond-like carbon, and nanodiamond, Philos. Trans. R. Soc. Lond. A 2004 (November 2004) 362. http://dx.doi.org/10.1098/rsta.2004.1452.

[7] A. Kriele, O.A. Williams, M. Wolfer, D. Brink, W. Müller-Sebert, C.E. Nebel, Tuneable optical lenses from diamond thin films, Appl. Phys. Lett. 95 (2009) 031905. http://dx.doi.org/10.1063/1.3183534(9).

[8] O.A. Williams, A. Kriele, J. Hees, M. Wolfer, W. Müller-Sebert, C.E. Nebel, High Young's modulus in ultra thin nanocrystalline diamond, Chem. Phys. Lett. 495 (2010) 84–89 (10.1016).

[9] A. Bongrain, E. Scorsone, L. Rousseau, G. Lissorgues, Ph. Bergonzo, Realisation and characterisation of mass-based diamond micro-transducers working in dynamic mode, Sensors Actuators B Chem. 154 (2) (June 20 2011) 142–149. http://dx.doi.org/10.1016/j.snb.2009.12.067 ISSN 0925-4005.

[10] Ji Won Suk, Shanthi Murali, Jinho An, Rodney S. Ruoff, Mechanical measurements of ultra-thin amorphous carbon membranes using scanning atomic force microscopy, Carbon 50 (6) (May 2012) 2220–2225. http://dx.doi.org/10.1016/j.carbon.2012.01.037 (ISSN 0008-6223).

[11] K. Small, W.D. Nix, Analysis of the accuracy of the bugle test in determining the mechanical properties of thin films, J. Mater. Res. 7 (1992) 1553.

[12] M. Delaunay, E. Touchais, Electron cyclotron resonance plasma ion source for material depositions, Rev. Sci. Instrum. 69 (1998) 2320–2324. http://dx.doi.org/10.1063/1.1148938.

[13] M. Delaunay, Permanent magnet linear microwave plasma source, Patent US 6319372 B1, 2001.

[14] J. Robertson, Diamond-like amorphous carbon (review article), Mater. Sci. Eng. R. Rep. 37 (4–6) (May 24 2002) 129–281.

[15] N. Sridi, B. Lebental, J. Azevedo, J.-C.P. Gabriel, A. Ghis, Electrostatic method to estimate the mechanical properties of suspended membranes applied to nickel-coated graphene oxide, Appl. Phys. Lett. 103 (2013) 051907. http://dx.doi.org/10.1063/1.4817301.